SCIENCE CHINA PRESS

SCIENCE CHINA Life Sciences
life.scichina.com link.springer.com
https://doi.org/10.1007/s11427-023-2458-1

RESEARCH PAPER

Longitudinal gut fungal alterations and potential fungal biomarkers for the progression of primary liver disease

Shiman Jiang[1†], Lvwan Xu[1†], Yanfei Chen[1], Zheyue Shu[2], Longxian Lv[1], Yuxi Zhao[1], Kefan Bi[1], Sisi Yang[1], Qiangqiang Wang[1] & Lanjuan Li[1*]

[1]State Key Laboratory for Diagnosis and Treatment of Infectious Diseases, National Clinical Research Center for Infectious Diseases, National Medical Center for Infectious Diseases, Collaborative Innovation Center for Diagnosis and Treatment of Infectious Diseases, The First Affiliated Hospital, Zhejiang University School of Medicine, Hangzhou 310003, China;
[2]Division of Hepatobiliary and Pancreatic Surgery, Department of Surgery, The First Affiliated Hospital, Zhejiang University School of Medicine, Hangzhou 310003, China

†Contributed equally to this work
*Corresponding author (email: ljli@zju.edu.cn)

Received 21 July 2023; Accepted 25 September 2023; Published online 26 February 2024

Liver disease, a major health concern worldwide, is a serious and progressive disorder. Herein, we not only established a mouse model of DEN+CCl_4-induced primary liver disease but also collected clinical human samples to investigate longitudinal alterations in the gut mycobiome. As liver disease advanced, gut integrity was disrupted, and the mycobiota was disturbed in the mouse models. The metabolites associated with hepatocellular carcinoma (HCC) differed from those associated with the cirrhotic phase as follows: levels of stercobilin and aflatoxin B1 dialcohol were reduced, while levels of triterpenoids, bafilomycin A1, and DHEA were increased in the HCC group. The abundance of the phylum *Chytridiomycota* increased as the chronic liver disease progressed and was then replaced by the phylum Ascomycota in HCC. Based on the results from clinical human samples, the genus *Candida* (Ascomycota) (in humans) and the genus *Kazachstania* (Ascomycota) (in mice) occupied a dominant position in the HCC group, while other fungi were depleted. The increased abundance of *C. albicans* and depletion of *S. cerevisiae* may be hallmarks of the progression of liver cirrhosis to early HCC. Moreover, the administration of *C. albicans* and *S. cerevisiae* in the LC-HCC progression could accelerate or retard the progression of HCC. Therefore, gut fungi have the potential to serve as a noninvasive clinical biomarker and even a treatment method.

gut mycobiome | liver disease | longitudinal studies | hepatocarcinogenesis | fungal biomarker

INTRODUCTION

Given its increasing incidence rates and association with long-term treatment, liver disease has developed into a major health burden worldwide (Wang et al., 2021). The common end stage of chronic liver disease is liver cirrhosis (LC) (Tonon et al., 2021), which may progress to hepatocellular carcinoma (HCC) (Qi et al., 2021) or decompensation (Acharya and Bajaj, 2021). Primary liver cancer (PLC) is the fourth leading cause of cancer-related death worldwide (Villanueva, 2019). By 2025, the prevalence of liver cancer has been estimated to be over one million globally, among which HCC is expected to account for approximately 90% of PLCs (Llovet et al., 2021). With hepatitis B vaccination and the control of hepatitis B and C, the number of hepatitis virus-induced liver cancers has decreased, which means that other factor-induced liver cancers are vital. The relationship between different states of liver disease and the gut microbiome together with its metabolic production during the onset and development of HCC has been confirmed by multiple studies. Yu and Schwabe, (2017) summarized the relationship between HCC and intestinal microecology, they proposed that the gut microflora and the gut-microbe-liver axis can act forward or backward on hepatocarcinogenesis.

To date, several studies have confirmed that the microbiota and its metabolites play significant roles in the progression of LC-HCC. Through the detection of a total of 419 samples (healthy controls, cirrhosis patients and early-stage HCC patients) by using MiSeq sequencing, our group found that the frequency of Actinobacteria in the early stage of HCC is more than that in LC (Ren et al., 2019). Thus, analysis of the bacterial genome in feces can act as a tool for noninvasive biomarkers for detecting early-stage HCC. Similarly, the bacterial flora and bacterial load of the HCC tumor microenvironment are progressively being investigated. Our team recently investigated the metabolites and genetic alterations between HCC and intratumoral bacteria (Xue et al., 2022). By longitudinal detection, hepatocytes from hepatic inflammation that develop into HCC in a stepwise manner are more likely to undergo damage and senescence (Rey et al., 2017). However, the gut flora and metabolism at various stages of liver disease have still not been described (Bi et al., 2021). Moreover, the changes in the microecology of the gut during the occurrence and development of different diseases are different and significant.

However, the role of the gut mycobiome in the development of liver diseases has not yet been investigated in depth. Most studies in this context were almost all restricted to alcoholic liver disease (Lang et al., 2020; Zeng et al., 2023a; Zeng et al., 2023b), and few studies were conducted to determine the relationships between the gut mycobiome and liver diseases. Since gut microbial biomarkers of liver diseases were found, the variations in gut fungi that occur during the progression of nonviral liver diseases in humans and rodents have remained unclear, and the

potential of fungal biomarkers and therapeutic targets remains to be further explored. Scientists have also proposed the necessity of investigating fungal compositional changes in liver diseases (Szóstak et al., 2023).

In this study, we investigated the dynamic evolution of the intestinal microecology and the gut-liver axis through different stages of liver disease: acute hepatitis (AH), chronic hepatitis (CH), LC and HCC. We set up mouse models of diethylnitrosamine (DEN)-induced and carbon tetrachloride (CCl_4)-promoted hepatocarcinogenesis to map disease variability profiles, depending on the strength of changes in the gut microbiome and metabolite dynamics.

RESULTS

The morphological, histological, and biochemical changes in the liver indicated the successful establishment of the CON-AH-CH-LC-HCC continuous model

After a combination of DEN and CCl_4 intraperitoneal injections, the DEN- and CCl_4-induced hepatocarcinogenesis model was successfully established (Figure 1A). Overall, 5 stages of chronic liver disease development were recorded and studied. As expected from their gross morphology (Figure 1B), the visceral and diaphragmatic surfaces of healthy liver samples appeared uniformly soft, with smooth contours and homogeneous textures. In particular, we observed that numerous white spots were homogeneously present in the gross liver surface of the AH stage. As the disease progressed to CH, the liver showed mild macroscopic swelling and a pale color. In the early to middle stages of cirrhosis, the enlarged size of the liver, the thicker shape of the lobes, the blunt edge of the liver, the brittle texture, and the granular surface became apparent. The disease progressed further until the sixth month, when significant solitary or multiple hepatocarcinoma was observed and characterized by several varying sizes of tumors on the liver surface.

Iconic histopathological alterations in hepatic tissue associated with liver disease progression were further characterized by hematoxylin and eosin (H&E) staining (Figure 1C). In contrast to normal liver pathology, the bridging necrosis in zone III, near the central vein, exhibited a banding distribution with inflammatory cell infiltration during the AH phase. In addition to bridging necrosis, hepatocyte ballooning, inflammatory cell increase, and lobular structural disorder also occurred during the CH phase. Furthermore, we observed a capsule of fibrous tissue surrounding a tubercle forming pseudolobules. In the HCC group, both HCC tissue and paracancerous tissue were evident with hepatocellular ballooning, high edema, steatosis and necrotizing foci. Numerous colonies were found in the portal area. Ki-67 staining and Sirius red staining were used to assess cell proliferation and hepatic fibrosis, respectively, suggesting a more distinct disease stage. F4/80 immunohistochemical staining clearly showed a random distribution of macrophages within the hepatic sinusoid.

However, liver disease progression can also be reflected by liver function measurements. Liver enzyme (alanine aminotransferase (ALT) and aspartate aminotransferase (AST)) levels in AH mice were dramatically elevated (Figure 1D). Throughout the other four groups, we found significant increases in serum ALT and AST levels in the CH and HCC groups compared with the normal group. Total bile acid (TBA) levels were significantly elevated in the AH and CH groups, indicating that liver cells were damaged.

Mycobiota distributions shifted significantly in the hepatocarcinogenesis process

In the development of liver cancer, the composition and proportion of the gut mycobiota changed significantly. The α-diversity results according to Chao1, Shannon, and Simpson index analysis are displayed in Figure 2A. We observed that the mycobiota diversity of the HCC stage compared to the other disease stages was significantly reduced. In addition to α-diversity, which illustrates within-sample biodiversity, β-diversity reflects intergroup diversity differences. PCoA plots based on binary Jaccard distance (R=0.2731, P=0.001), Bray-Curtis distance (R=0.5843, P=0.001) and Euclidean distances (R=0.5563, P=0.001) all exhibited obvious between-group differences (Figure 2B). The relative abundance of certain fungal phyla, including Ascomycota, Chytridiomycota, and Basidiomycota, varied greatly at the different stages of liver disease (Figure 2C). At the consecutive stages of healthy, AH, CH, LC and HCC, the dominant phyla were variable. The results illustrated the ratio of representative phyla with relatively high abundance in certain groups. Eventually, Ascomycota became the only predominant phylum. In addition, linear discriminant analysis effect size linear discriminant analysis effect size (LefSe) analysis was performed to indicate the differential fungal composition enriched in the five phases (Figure 2D). The cladogram illustrates the extremely important status of *Saccharomyces* in the later stages of disease development. Additionally, we observed a rapid increase in *Kazachstania pintolopesii* and a noticeable decrease in *Saccharomyces cerevisiae* and *Aspergillus heterocaryoticus* in the HCC stage (Figure 2E).

Before the onset of the disease, intact gut tissue structures possessed regularly arranged microvilli and glands (Figure 3A). When acute inflammation occurred, goblet cell numbers significantly decreased, and inflammatory cells infiltrated the lamina propria. In addition to the shriveled, smaller, and more cluttered intestinal villi, the number and secretion of goblet cells were significantly reduced. In the immunofluorescence labeling of claudin-3 (Figure 3B), we found that intestinal integrity worsened, which is consistent with hepatic disease. Along with the changes at different stages of the disease, not only gut integrity but also intestinal secretion function was altered (Figure 3C). In addition, the colonic transcriptome analysis of different stages was performed for further gene expression profile investigation. In the principal component analysis (PCA) (Figure 3D), a significant intergroup difference was found, indicating an altered gene expression at different stages of liver diseases. And in Figure 3E, we observed the changes in transcriptomic gene expression. The top 50 genes with the smallest P-values were studied, and we observed not only a similarity between group CON and group AH, but also a difference between group CON and group HCC.

Fecal metabolic profiling showed obvious alterations at different stages of hepatocarcinogenesis

Obvious differences in metabolic substances were observed between separate groups according to orthogonal partial least-squares-discriminant analysis (OPLS-DA) data, which are depicted in Figure 4A. In general, over 20 kinds of intragroup

https://doi.org/10.1007/s11427-023-2458-1

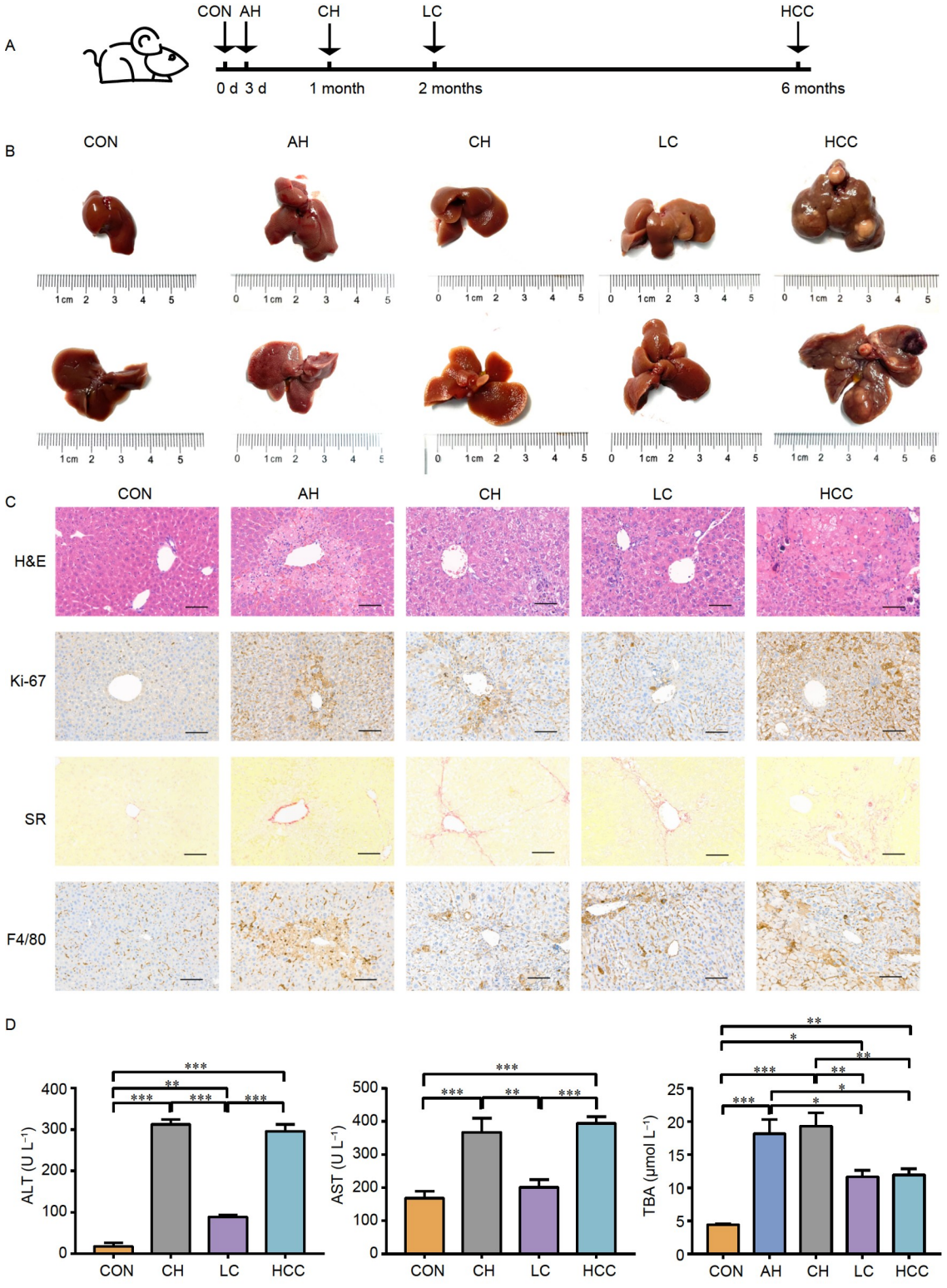

Figure 1. The establishment and characteristics of the CON-AH-CH-LC-HCC continuous mouse model at different stages. A, Establishment of the CON-AH-CH-LC-HCC continuous model. B, Changes in the appearance of the liver at different stages. C, H&E staining, Ki-67 staining, Sirius red staining and F4/80 immunohistochemical staining of the liver. scale bar, 100 μm. D, Comparisons of ALT, AST, TBA at different stages by liver function measurements. Data are presented as the mean±standard error of the mean (SEM). *, $P<0.05$; **, $P<0.01$; ***, $P<0.001$.

fecal differential metabolites were together displayed by heatmap clustering (Figure 4B). The contents of different metabolites varied greatly during different periods of liver diseases. At the final stage of HCC, we found that the contents of lovastatin acid, MG (18:2(9Z,12Z)/0:0/0:0)), 2α-(3-hydroxypropyl)-1α, 25-dihydroxy-19-norvitamin D3, allocholic acid, nutriacholic acid, and

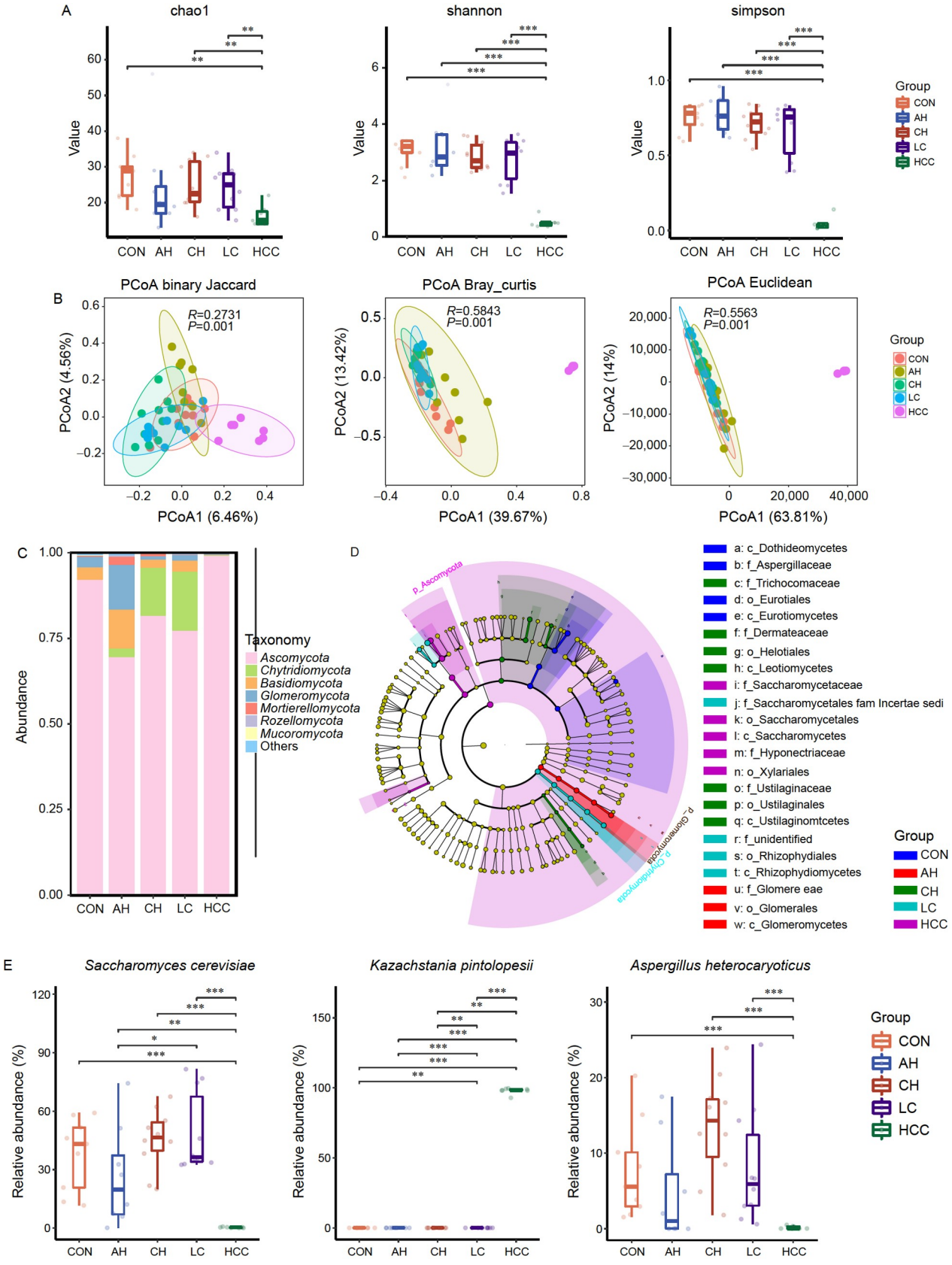

Figure 2. The composition of the gut mycobiota changed significantly during the development of liver diseases. A, α-diversity of Chao1, Shannon, and Simpson indexes at different stages. B, β-diversity was evaluated by PCoA plots based on binary Jaccard distance, Bray-Curtis distance and Euclidean distances. C, The change in the proportion of fungal phyla in each period. D, LefSe analysis. E, Relative abundance of *Kazachstania pintolopesii*, *Saccharomyces cerevisiae* and *Aspergillus heterocaryoticus* at five stages. Data are presented as the mean±SEM. *, $P<0.05$; **, $P<0.01$; ***, $P<0.001$.

https://doi.org/10.1007/s11427-023-2458-1

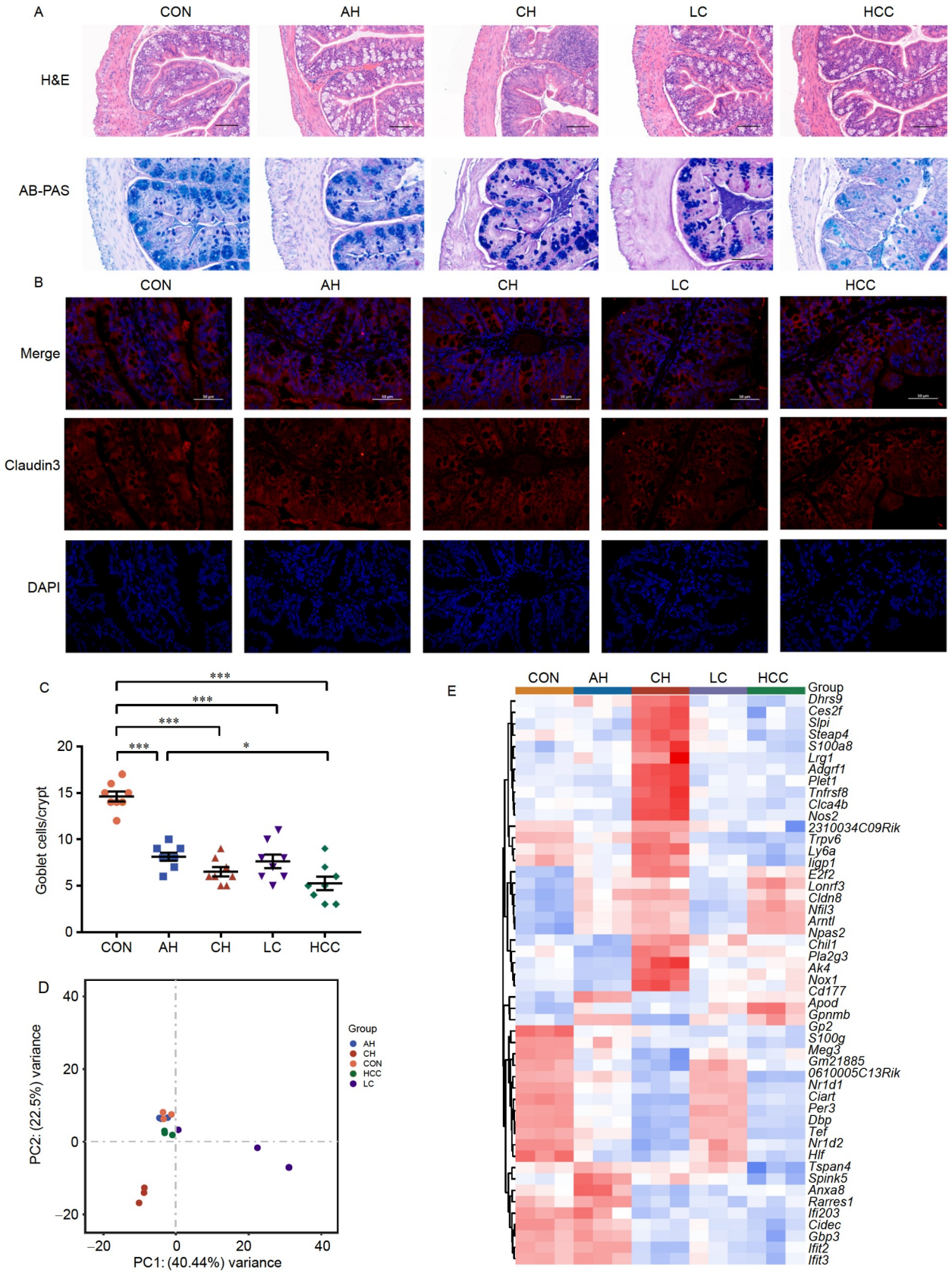

Figure 3. Colonic tissue damage occurred as the disease progressed. A, H&E staining and AB-PAS staining of the colon at different stages. scale bar, 100 μm. B, Immunofluorescence labeling of Claudin-3 (red) and DAPI (blue). scale bar, 50 μm. C, The AB-PAS rating. D, PCA analysis of colonic tissues among 5 phases. E, Expression of top 50 genes of transcriptome sequencing in CON, AH, CH, LC, and HCC groups. Data are presented as the mean±SEM. *, $P<0.05$; **, $P<0.01$; ***, $P<0.001$.

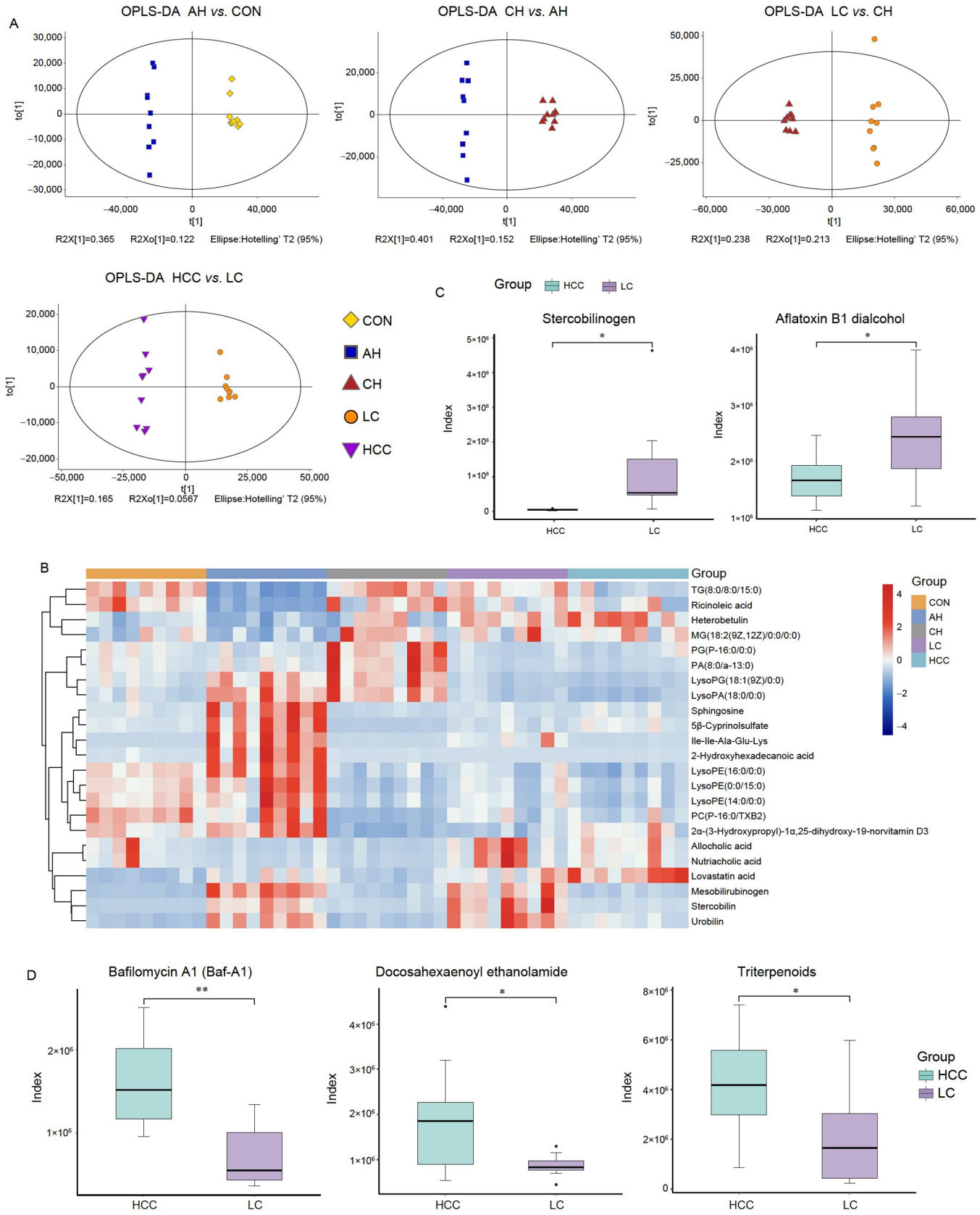

Figure 4. Fecal metabolic profiling changed in the process of CON-AH-CH-LC-HCC. A, OPLS-DA data showed differences in metabolic substances between separate groups. B, Heatmap clustering of obvious differential metabolites. C, Comparison of the contents of stercobilinogen and aflatoxin B1 dialcohol between HCC and LC. D, Comparison of the contents of Baf-A1, docosahexaenoyl ethanolamide, and triterpenoids between HCC and LC. Data are presented as the mean±SEM. *, $P<0.05$; **, $P<0.01$.

https://doi.org/10.1007/s11427-023-2458-1

heterobetulin in feces were elevated. Additionally, TG (8:0/8:0/15:0), PC (P-16:0/TXB2), LysoPE (16:0/0:0), LysoPE (0:0/15:0), and LysoPE (14:0/0:0) were reduced in end-stage liver disease. As shown in Figure 4C, a marked decrease was observed in the content of some metabolites, especially stercobilinogen ($P<0.05$) and aflatoxin B1 dialcohol ($P<0.05$). In distinct contrast, the contents of triterpenoids, bafilomycin A1 (Baf-A1) ($P<0.01$), docosahexaenoyl ethanolamide ($P<0.05$), protopanaxadiol ($P<0.01$), etc., increased significantly (Figure 4D).

To further reveal a potential interaction between the fecal mycobiome and metabolome, we conducted Spearman's correlation analysis on the top 10 differential fungal genera and top 20 differential metabolites (Figure 5A). At the genus level, *Kazachstania*, *Botrytis*, *Inocybe*, *Trametes*, *Aspergillus*, *Xerochrysium*, *Saccharomyces*, *Diutina*, and *Moesziomyces* were highly related to the majority of metabolite contents. Conversely, certain metabolites, especially 1,3,12-trihydroxycholan-24-oic acid, (22E)-3β-hydroxy-5α-chola-7,22-dien-24-oic acid, 3β, 7α, 12α-trihydroxy-5β-cholanoic acid, heterobetulin, L-leucine, and some lysophospholipids had significant correspondence with gut fungi. Among them, 1,3,12-trihydroxycholan-24-oic acid and 3β,7α,12α-trihydroxy-5β-cholanoic acid are cholic acid metabolites related to the host and microbiota that could function in antibacterial reactions and host immune modulation. In the association network diagram (Figure 5B), association lines showed that the genera *Kazachstania* and *Aspergillus* played pivotal roles in metabolite regulation.

In the mouse models, the potential factors that influence the changes in the gut microbiota during the carcinogenesis process were assessed. Due to the relatively few interfering factors, the relationship between the pathophysiological indicators of the mouse models and the dominant fungal species was investigated. Figure 5C displays the correlation between the top 8 most altered fungal species and indicators representing inflammation, proliferation, liver enzymes, and intestinal damage. The Spearman's rank correlation indicated that the AOD scores of Ki-67 and Sirius red staining were the most correlated indicators, which depicted the liver condition. Furthermore, strong correlations with those phenotypes were observed in *Aspergillus penicillioides*, *Saccharomyces cerevisiae*, and *Kazachstania pintolopesii*. However, the cause-effect relationship might be an interaction. For instance, during the progression of a disease, the phenotypes worsen, and the gut mycobiome undergoes alterations. Subsequently, the gut mycobiome can exacerbate or ameliorate liver disease conditions, including phenotypes.

Gut mycobiota shifted in human feces during AH-CH-LC-HCC longitudinal disease progression and potential fungal biomarkers

To further validate the gut fungal structural variation in mice, we carried out clinical sample collection and mycobiome detection. A total of 80 fecal samples from hospitalized patients were collected, and after screening, 39 samples (HCC:LC:CH:AH=6:14:8:11) were subjected to internal transcribed spacer (ITS) sequencing (Figure 6A). The Shannon index, which was used to evaluate species richness, exhibited distinct decreases in HCC and AH patients (Figure 6B). It was clearly visible that every group was distant from each other in the PCoA of Bray-Curtis distances (PC1 10.3%, PC2 8.96%, $P<0.05$) (Figure 6C). The relative abundances of fungal phyla during different stages of liver diseases showed a disruption of Ascomycota in HCC (Figure 6D), which was similar to the results of the mouse models. Furthermore, LefSe analysis was conducted, and then the significantly different species were studied (Figure 6E). In the CH stage, the abundance of dominant fungi displayed an obvious distinction. Subsequently, the gut fungal feature of LC patients was not evident. However, the HCC stage was dominated by several representative fungi, such as the *Candida* genus, *Phaeosphaeria* genus, and *Saccharomycetales fam. Incertae sedis* species. In addition, the *Candida* genus had a higher relative abundance in the HCC group than in the LC group (Figure 6F).

In addition, metabolomic analysis of human fecal samples was performed. OPLS-DA revealed significant intergroup differences among liver disease phases (Figure 7A). After the removal of the interferences of food and drug, the residual top 50 differential metabolites were listed in Figure 7B. However, because of the complexity of dietary patterns and human diseases, there is no consistency in the metabolic relationships between mice and humans.

Furthermore, indicator analysis was conducted to screen fungal biomarkers (Figure 7C). The *Candida* genus may become one of the biomarkers of liver cancer, and the *Herpotrichia* genus may be a warning sign of the progression of liver disease. Random forest analysis (Figure 7D) found that the genus *Candida* might play a major role in these diseases, far more so than the genus *Saccharomyces* and other fungal genera.

Supplementation with *C. albicans* and *S. cerevisiae* can either promote or retard the progression of cancer

To investigate the role of *C. albicans* and *S. cerevisiae* in LC-HCC progression, LC-stage mice were orally administrated with *C. albicans* and *S. cerevisiae* until HCC formation (Figure 8A). After sacrifice, the tumorigenesis of livers was embodied in the overall diameter of liver cancers. As is shown in Figure 8B, the tumor formation rate in the CA group was lower than that in the HCC group, contrary to the results in the SC group. Moreover, the status of livers (Figure 8C) and colons (Figure 8D) were estimated by pathology. By combining the results of Ki-67 (cell proliferation) and F4/80 staining (macrophage exhibition), we found that *S. cerevisiae*-treated mice had less inflammation and lower tumor incidence, while *C. albicans*-treated mice exhibited more severe disease. The integrity of colonic villi and intestinal barrier function were ameliorated in the SC group, while inflammation and disruption were aggravated in the CA group. All these results provided a foundation for our conclusions.

DISCUSSION

Liver disease is a serious and increasingly common health issue, affecting millions of people worldwide. More than 800 million people are afflicted with chronic liver disease, which can develop into LC and HCC (Trebicka et al., 2021). The final stage of liver damage, inflammation, and compensatory hepatocyte proliferation is cirrhosis, which has been associated with approximately 80% of HCC cases (Llovet et al., 2016). A frequently applied DEN- and CCl_4-induced mouse model was established to deduce fibrosis-associated liver cancer, which reflects the state of disease progression in HCC patients (Chappell et al., 2014). During continuous intraperitoneal carbon tetrachloride injection, our findings demonstrated that hepatic inflammation, fibrosis,

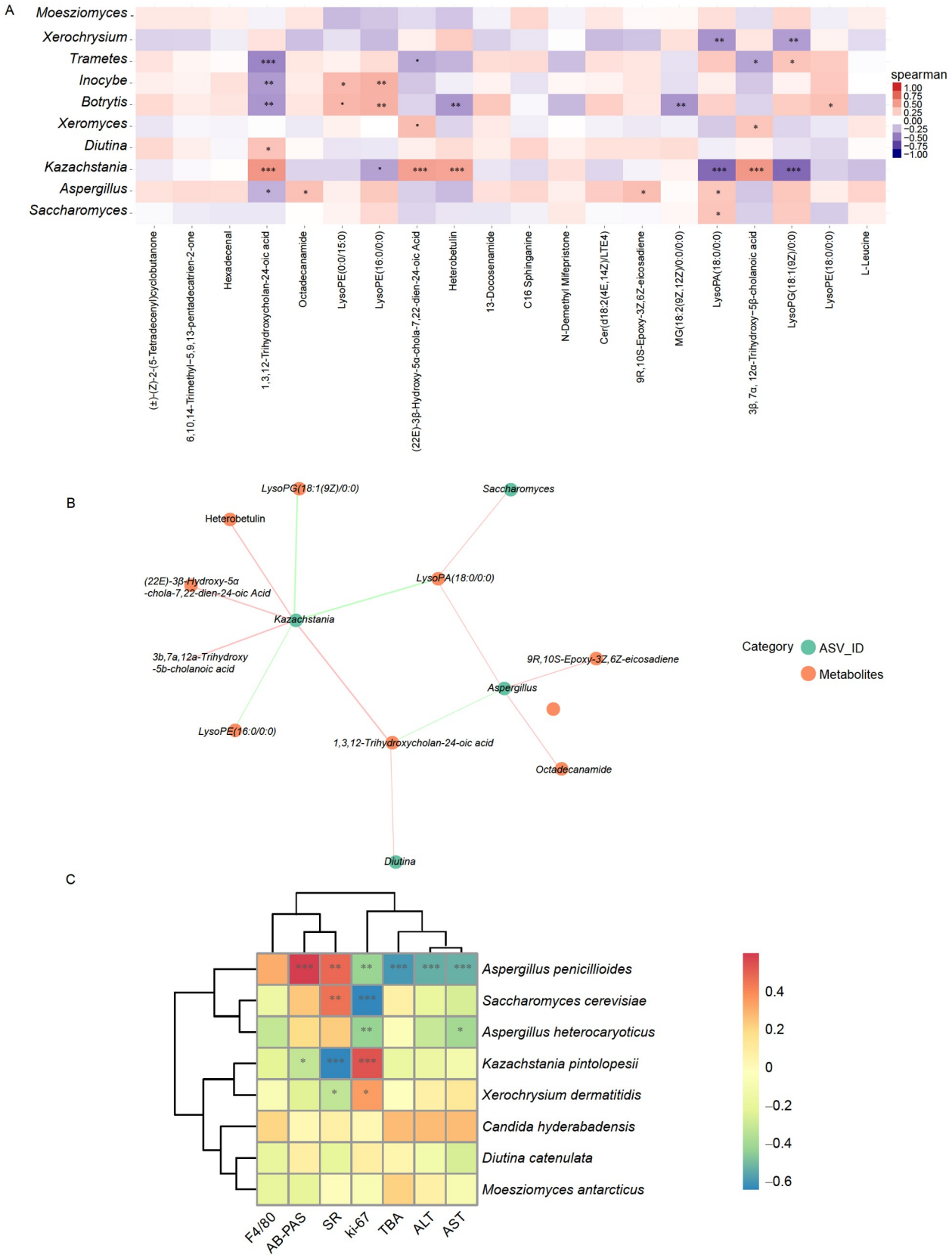

Figure 5. Potential interactions between the fecal mycobiome and metabolome. A, Spearman's correlation analysis of the top 10 differential fungal genera and the top 20 differential metabolites. B, The predicted association network between the fecal mycobiome and metabolome. Green: ASV_ID, Red: Metabolites. C. The Spearman's correlation among the top 8 most altered fungal species and the alterations in the liver and colon. Correlations with $P<0.05$ and $r>0.8$ are indicated as significant. Red (positive), blue (negative), and yellow (no correlation) colors are applied for representation. *, $P<0.05$; **, $P<0.01$; ***, $P<0.001$.

https://doi.org/10.1007/s11427-023-2458-1

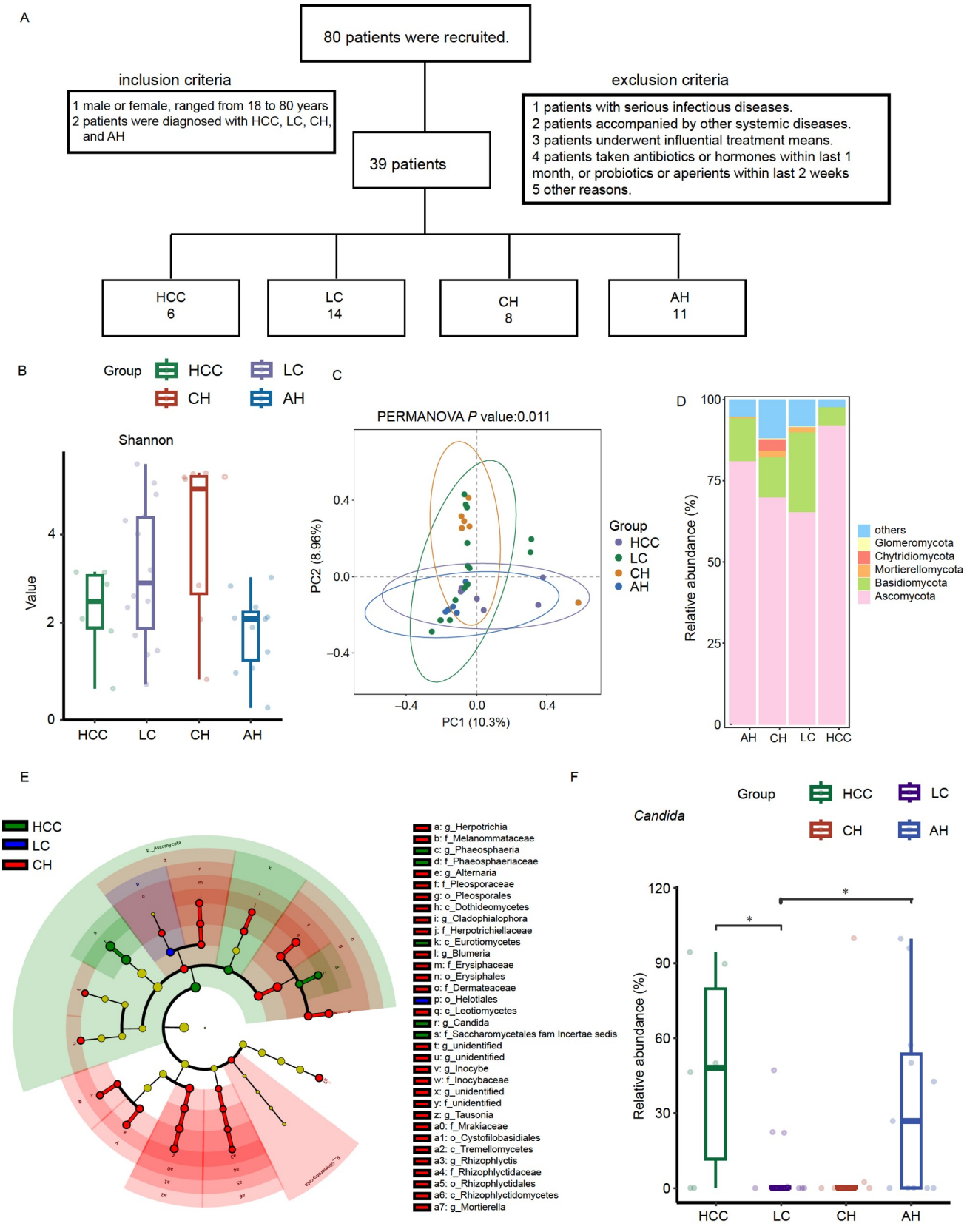

Figure 6. Changes in intestinal fungi were observed at different stages in clinical samples. A, Screening criteria and procedures for clinical samples. A total of 39 patients were analyzed, including 6 with HCC, 14 with LC, 8 with CH, and 11 with AH. B, Shannon indexes at different stages. C, PERMANOVA at different stages (*P* value: 0.011). D, Relative abundance of fungal phyla at different stages. E, LefSe analysis of HCC (green), LC (blue), and CH (red). F, The relative abundances of the genus *Candida* at different stages. Data are presented as the mean±SEM. *, $P<0.05$.

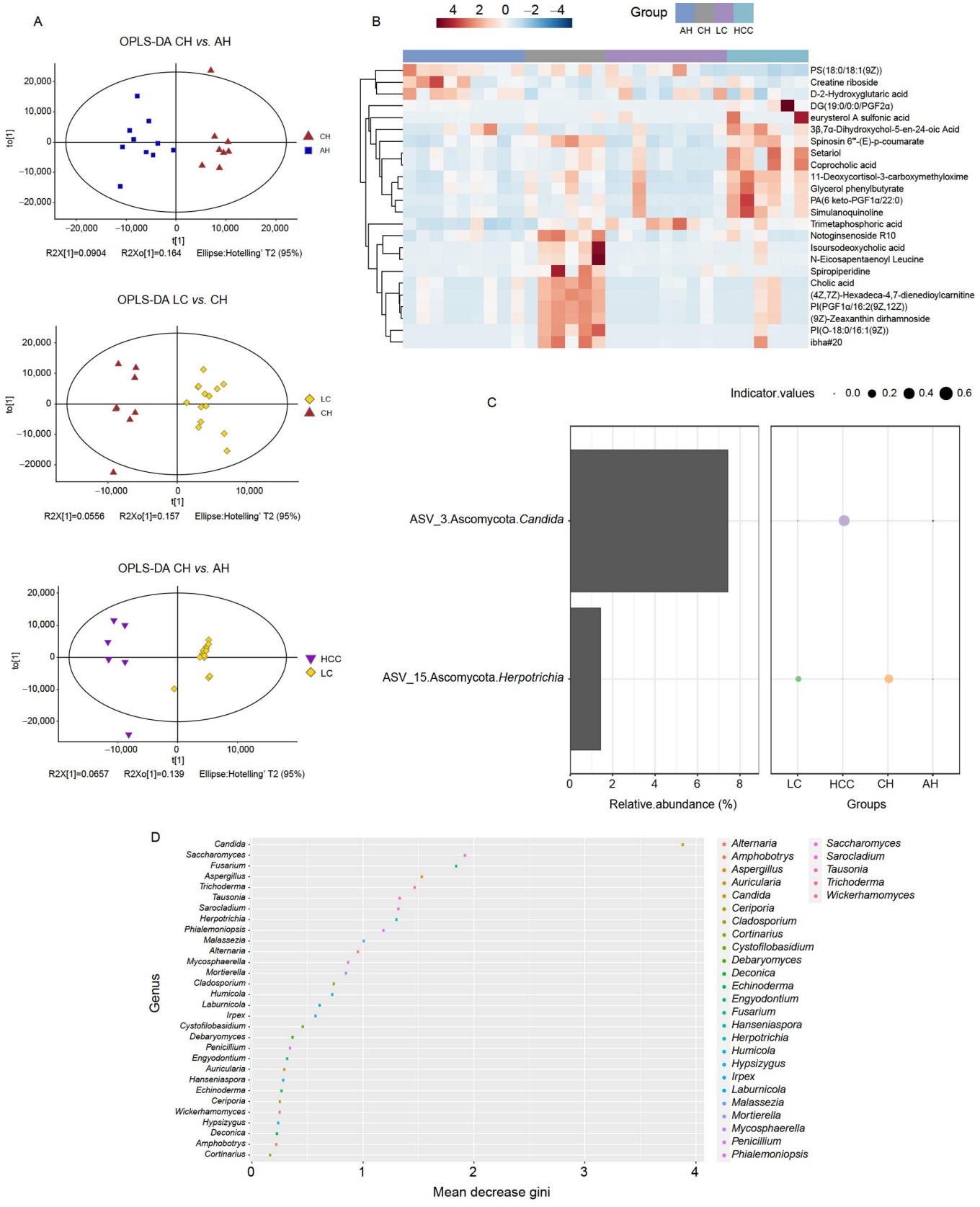

Figure 7. Indicator species and predictive biomarkers at different stages. A, OPLS-DA data showed differences in metabolic substances between separate human groups. B, Heatmap clustering of obvious differential metabolites of human feces. C, Indicator analysis: representative genera that have a certain impact on the status. Bar graphs show individual ASV relative abundances. The abscissa of the bubble plot represents the groups, with the bubble size representing indicator values. D, Random Forest analysis: the abscissa represents the criterion of importance, and the ordinate represents the top 30 genera.

https://doi.org/10.1007/s11427-023-2458-1

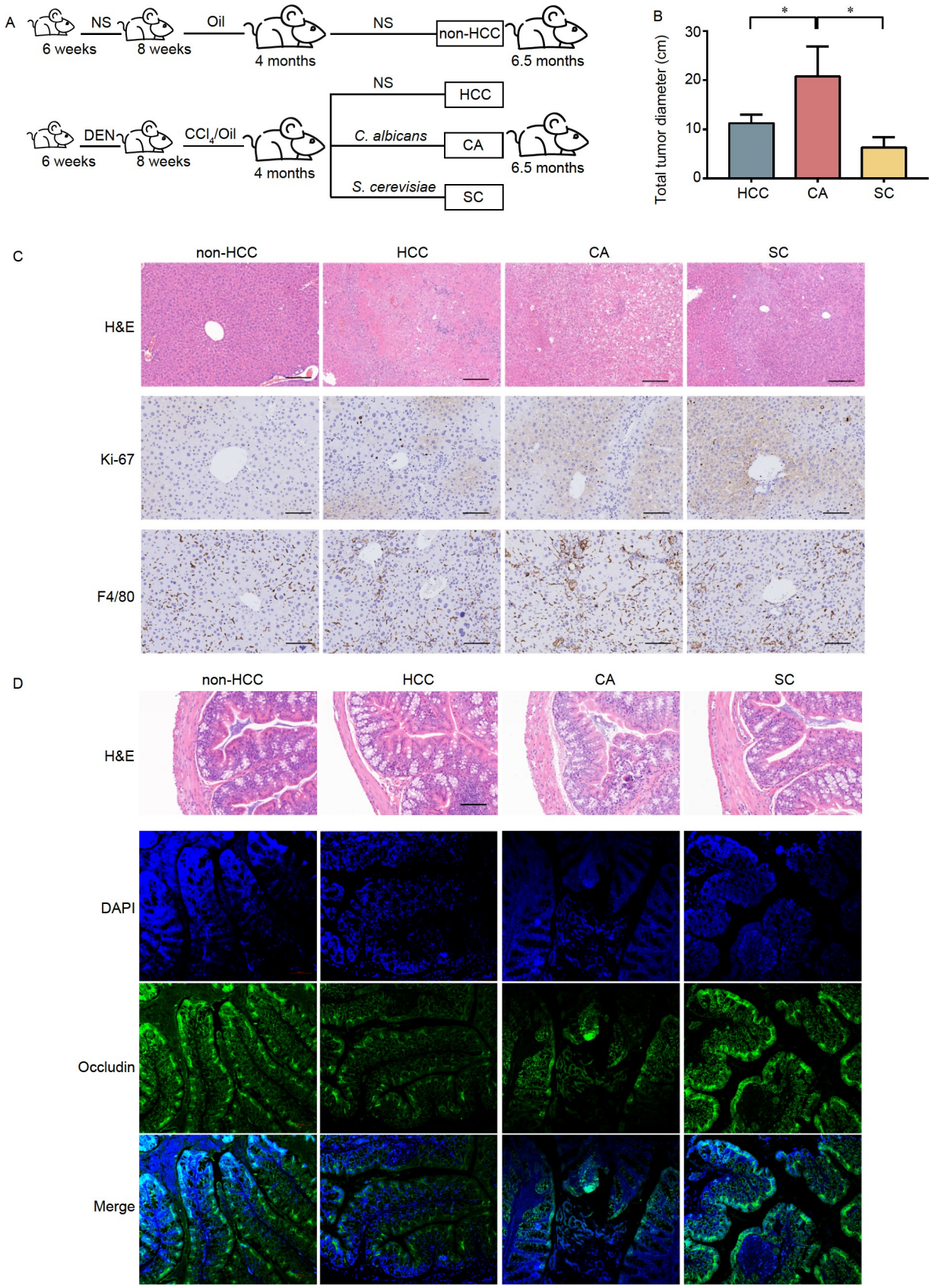

Figure 8. Supplemented with *C. albicans* and *S. cerevisiae* for result verification. A, Schematic diagram of mouse models and interventions. B, Total diameters of tumor (cm) in the HCC, CA, and SC groups. C, H&E staining and Ki-67, F4/80 IHC staining of livers in the non-HCC, HCC, CA, and SC groups. D, H&E staining (Scale bar, 50 μm) and occludin and ZO-1 IF staining (Scale bar, 100 μm) of colons in the non-HCC, HCC, CA, and SC groups. Data are presented as the mean±SEM. *, $P<0.05$.

function, immune cell recruitment, and apoptosis were consistent with the progression of liver diseases. Immediately after exposure to DEN, hepatocyte apoptosis and macrophage recruitment occurred (Liang et al., 2019), followed by cirrhosis of the liver at 3 months and HCC at 6 months.

In the multistep process from normal liver, AH/CH, and ultimately cirrhosis, or even HCC, the gut microbiota may play significant roles (Ling et al., 2022; Roderburg and Luedde, 2014). Through the gut-liver axis, the gut microbiome and the liver interact in numerous ways. For instance, metabolites from the intestine into the liver (Liu et al., 2022b), *Enterococcus faecalis* (Iida et al., 2021), *Stenotrophomonas maltophilia* (Liu et al., 2022a), *Lactobacillus reuteri* (Chen et al., 2022), etc., all contribute to the formation of liver cancer. By 16S rRNA gene sequencing, one research group found a significant reduction in gut microbial diversity in the liver tissue of HCC, while the abundance of *Stenotrophomonas maltophilia* increased inversely. *S. maltophilia* activated the TLR-4-mediated NF-κB signaling pathway, which facilitated cirrhosis and tumor formation (Liu et al., 2022a). Overall, major research attention has been focused on the highly abundant bacterial microbiome, and the potential role of gut fungi has been neglected. In particular, intestinal fungal detection and treatment have not been routinely applied in clinical applications. Therefore, we further explored the variability and possible effects of the gut mycobiota on liver disease. During the occurrence and development of many chronic progressive diseases, the structure and composition of the gut microbiota are shifted significantly. Investigators have found that the gut microbiota profile has a unique representation for each disease, forming its disease pattern. For PLC, the current focus is almost exclusively on the gut bacteriome and seeks to represent the entire gut microbiome. Researchers have established a gut bacteriome-based diagnostic model for liver cancer (Deng et al., 2022). Several researchers have proposed the necessity of microbial biomarkers in HCC independent of clinical and radiological assessments in the background of LC (Albhaisi et al., 2021).

However, whether the intestinal mycobiota exhibits predictable changes remains to be determined. First, we performed a comprehensive evaluation of the intestinal mycobiota, fecal metabolome, intestinal integrity, etc., in mouse models of initiation and development of DEN- and CCl_4-induced liver cancer. First, anomalous goblet cell morphology and a reduction in the number of goblet cells were observed in the exacerbation of liver disease. Claudin-3, one of the known tight junction proteins, represents the mucosal integrity and barrier function of the gut (Garcia-Hernandez et al., 2017). With the exacerbation of the liver profile, the expression of claudin-3 decreased gradually. Translocation of intestinal microbes was found during the disease, which is a sign of chronic liver disease and a cause of liver fibrosis and inflammation (Dapito et al., 2012). To the best of our knowledge, the gut-liver axis plays a critically important role in association modification. We sought not only to determine the key fungi and metabolites involved in the progression of liver diseases over time but also to investigate longitudinal alterations in the gut mycobiome. Observable changes in the fungal spectrum were noted during liver disease, culminating in a marked reduction in the diversity of mycoflora in HCC mice compared with other disease stages. The phylum Chytridiomycota was identified during the liver disease progression period but disappeared abruptly in the HCC stage. *Kazachstania pintolopesii* increased considerably in HCC mice and was previously reported to induce inflammatory reactions in mouse colon tissues through IL-17A/IL-17RA signaling (Zhang et al., 2022b). In contrast, the contents of *Saccharomyces cerevisiae* and *Aspergillus heterocaryoticus* in HCC mice were extremely low. β-D-glucans, yeast cell wall components from *S. cerevisiae*, have antitumor functions in liver cancer by impairing autophagosome and lysosome function (Wang et al., 2020a).

During liver disease, not only are the colonic mucus layer and tight-junction proteins gradually destroyed, leading to translocation of the colony, but the composition of gut fungi and metabolites varies considerably. Relatedly, metabolic products of the gut in liver disease progression also have representative substances in each period. In the present study, liver disease-specific metabolomic profiling was carried out. Some fecal metabolites are highly expressed in the common state but have low expression with disease status. For example, TG (8:0/8:0/15:0) and ricinoleic acid (antimicrobial properties (Park et al., 2020)) exhibited low expression in AH and HCC, while LysoPE (16:0/0:0), LysoPE (0:0/15:0), LysoPE (14:0/0:0), and PC (P-16:0/TXB2) had low expression in CH, LC, and HCC. In turn, some metabolites were rarely present in feces representing a healthy state but were clustered in feces representing states of liver disease. Lovastatin acid, which is produced by several strains of fungi, such as *Aspergillus terreus* (Wu et al., 2023), *Fusarium nectrioides* (Manogaran et al., 2023), and *Hypsizygus marmoreus* (Kala et al., 2022), was more highly expressed in feces during the LC and HCC phases. On the one hand, it has lipid-lowering properties; on the other hand, it can induce tumor cells to undergo apoptosis (Kah et al., 2012). We found that the content of stercobilin and aflatoxin B1 dialcohol in feces dropped sharply when LC evolved into HCC. Stercobilin is a kind of microbial metabolite that can be reabsorbed into the blood system and then induce inflammation (Sanada et al., 2020). In addition, aflatoxin B1 dialcohol is well known for its carcinogenic and toxic effects on the liver. Triterpenoids, bafilomycin A1, and dehydroepiandrosterone (DHEA) are instead higher at the final step. Associated with fungi, triterpenoids are not only liver-protective but also anticancer and anti-inflammatory (Li et al., 2023b). As an autophagy inhibitor, bafilomycin A1 may slow the progression of liver diseases (Thoen et al., 2011). DHEA, which naturally and endogenously exists in the body, inhibits the progression of tumors (Augimeri et al., 2023) and inflammation (de Bus et al., 2021). In human samples, the alteration of fecal metabolites was not the same as above. The levels of bile acids (3β,7α-dihydroxychol-5-en-24-oic acid, coprocholic acid) and ammonia-lowering metabolites (glycerol phenylbutyrate) were significantly increased in HCC patients, illustrating unfavorable states of end-stage liver disease (Jia et al., 2023).

Certainly, we admit that mouse models have potential and inherent limitations. In addition to the mouse model, validation was performed with human samples. There was also a variation law for the human keystone gut fungus corresponding to the mouse. Consistent with this, the genus *Candida* and the species *Saccharomycetales fam. Incertae sedis* may be biomarkers of the HCC phase by LefSe analysis. At the final stage of hepatocarcinogenesis, the species and contents of fungi changed dramatically, which mainly manifested as a noticeable increase in *Candida*. Of these, the genus *Candida* has been discovered to be involved in the pathogenesis of numerous hepatobiliary disorders (Hartmann and Schnabl, 2023). In addition, the gut mycobiomes

https://doi.org/10.1007/s11427-023-2458-1

of common populations, patients with LC, and patients with different stages of liver cancer were identified by Wang's and Deng's groups (Zhang et al., 2023), which can further complement and strengthen the results related to the gut mycobiome of liver diseases. An experiment was subsequently performed to confirm the status of *C. albicans*. Colonization of the intestinal tract of mice with *C. albicans* was confirmed to promote the formation of HCC. The heterogeneity of liver diseases, multiple comorbidities, dietary exposure, or even social activities in human patients all lead to the instability of clinical findings. Therefore, the alterations in the mycobiome of mice and humans are complementary and congruent, and both results should be considered.

Mycobiota keeps continually shifting and changing from cradle to grave, which is crucial for human health. Fungal microbial dysbiosis may play a role in the pathogenesis of intestinal and other diseases (Zhang et al., 2022a). Commensal enteric fungi may beneficially affect local tissues and boost antimicrobial systemic immunity (Jiang et al., 2017). Bajaj et al. (2018) collected fecal samples from cirrhosis patients and healthy volunteers and then found intestinal fungal dysbiosis in patients, which varied with the usage of antibiotics and proton pump inhibitors. During the late stages of hepatocarcinogenesis, eliminating the normal flora suppresses the progression of liver cancer (Dapito et al., 2012). The elimination of fungi, e.g., using terbinafine (Zhang et al., 2021), itraconazole (Wang et al., 2020b), and ketoconazole (Chen et al., 2019), can suppress tumor growth in HCC preclinical models. Apart from exploring the critical fungi and their metabolites in longitudinal liver diseases over time, we also focused on the LC-HCC process. Combining the ITS results from the mouse model and the human sample, *Kazachstania pintolopesii* and *Candida albicans* showed a sharp increase throughout LC-HCC. In addition, *K. pintolopesii* is a common intestinal colonizer in rodents, but *C. albicans* is present in the human intestinal system (Naglik et al., 2008). Thus, *C. albicans* is a major risk factor in LC-HCC progression. In addition, this work not only identified disease indicators through fungal distribution patterns but also provides the foundation for balancing the intestinal mycoecology of liver diseases for further fungal treatment. The HCC stage might be postponed by increasing the content of *S. cerevisiae* and depleting the content of *C. albicans* before irreparable disease outcomes.

Further studies were conducted to determine whether *S. cerevisiae* and *C. albicans* play a critical role in hindering or promoting the progression of LC-HCC. After administration of *S. cerevisiae* and *C. albicans*, the overall tumor diameter, progression of liver diseases, colonic barrier integrity and tight junction proteins of mice were ameliorated or aggravated. All these results support the alterations in fungal shifts in the progression of liver diseases. Additionally, the effects of *C. albicans* in LC-HCC were initially studied (Liu et al., 2022c), and the findings were under our conclusion. Therefore, gut mycobiota can not only act as biomarkers for the progression of liver diseases, but also potentially serve as a prevention or treatment option.

This study had some potential limitations. First, the sample size of clinical patient feces might be further increased, and the collection cycle could be further expanded. Second, we acknowledge the inevitable differences in the dominant colonies of the mouse model and the human body as well as the myriad factors affecting the human gut ecosystem, therefore both results should be taken into account. Third, the enormous cost of metagenomic testing or ITS sequencing puts pressure on clinical practice, and the detection of iconic fungi can be a tendency.

In conclusion, both DEN+CCl_4-treated carcinogenesis mouse models and human samples of different stages of liver diseases were applied to explore longitudinal gut mycobiome alterations. The phylum *Chytridiomycota* increased in the pathogenesis of chronic liver diseases, while the genus *Candida* (*Ascomycota*) (in humans) or the genus *Kazachstania* (*Ascomy-Ascomycota*) (in mice) occupied a dominant position in the HCC stage. Gut fungal surveillance has the potential to function as a noninvasive biomarker. We propose that exacerbation of *C. albicans* and depletion of *S. cerevisiae* are a hallmark of LC to early HCC. The ratio of *C. albicans*:*S. cerevisiae* may be a clinical indicator of HCC that needs to be identified and validated. Finally, our study provides the basis for retardation of disease progression in the chronic liver disease phase by changing the gut fungal fraction.

MATERIALS AND METHODS

Clinical specimen assessment and collection

We collected fresh fecal samples from inpatients at the AH, CH, LC and HCC disease stages, evaluated by clinical assessment or physician evaluation from 2022 to 2023. The inclusion criteria were (i) male or female patients, ranging from 18 to 80 years, and (ii) patients diagnosed with HCC, LC, CH, and AH. The exclusion criteria were (i) patients with serious infectious diseases, such as HIV infection, viral hepatitis, and syphilis; (ii) patients with other systemic diseases, such as intestinal disorders and hematological disease; (iii) patients who underwent radiotherapy, chemotherapy, and any other influential treatment means; (iv) patients who took antibiotics or hormones within the last 1 month or probiotics or aperients within the last 2 weeks; and (v) patients who declined to participate or were already enrolled in other clinical trials. All participants signed an informed consent form. Feces were collected and frozen at −80°C until analyses. This study was reviewed and approved by the Clinical Research Ethics Committee of the First Affiliated Hospital, Zhejiang University School of Medicine.

Animal model construction and sample collection

Five-week-old male Balb/c mice were kept in the animal experimental center of the First Affiliated Hospital of Zhejiang University. Under the condition of constant temperature and a 12-h light-dark cycle, mice had ad libitum access to water and food. After a week of adaptive feeding, mice were injected intraperitoneally with DEN at a concentration of 100 mg kg^{-1} body weight. Then, 2 weeks later, carbon CCl_4 intraperitoneal injections (0.5 mL kg^{-1}, 25% olive oil suspension) were applied twice per week to build different stages of liver disease according to previously reported protocol (Li et al., 2015). All the models comprised the following five phases: normal (0 d, before DEN injection), acute hepatitis (3 d, after DEN injection), chronic hepatitis (1 month), liver cirrhosis (2 months), and hepatocellular carcinoma (6 months). Then, the mice (n=10) were anesthetized and sacrificed at the abovementioned time points. Feces, blood, liver, colon, and ileum were collected for further investigation.

Liver function

Various indicators of liver function, including AST and ALT, and TBA, were assayed by employing the Hitachi 7600-210 automatic analyzer (Hitachi, Japan).

Histopathology, IHC and immunofluorescence

After fixation with 10% neutral buffered formalin, liver and colon samples were paraffin-embedded and 2-μm-sectioned. H&E staining of liver fixation was used to assess the progression of liver disease, while H&E staining of colon specimens was used to evaluate gut structural integrity and changes. In addition, hepatic fibrogenesis was evaluated by Sirius red staining (Ma et al., 2023). Hepatic cell proliferation and Kupffer cells were evaluated by immunohistochemical analysis with anti-Ki-67 antibody [SP6] (Abcam, USA) (Li et al., 2023a) and recombinant anti-F4/80 antibody [EPR26545-166] (Abcam), respectively. Furthermore, Alcian blue-periodic acid-Schiff (AB-PAS) staining was performed to trace goblet cells according to previously described protocols (Gao et al., 2022). Sections from the proximal colon were used to explore tight-binding proteins by immunofluorescence. After being dewaxed and rehydrated, sections were incubated with claudin-3 antibodies purchased from Proteintech (USA) at 4°C overnight. In addition, secondary antibodies were combined with washed samples at room temperature for 1 h. After rinsing, the sections were sealed and then captured by a Nikon Eclipse Ci epifluorescence microscope (Nikon, Japan).

Fecal metabolomics analysis

Fifteen milligrams of feces, 400 μL of methanol-water mixture (v: v=4:1, including 2-chloro-l-phenylalanine, 4 μg mL^{-1}), and two steel beads were transferred into tubes. After precooling in a −40°C refrigerator and grinding at 60 Hz for 2 min, each sample was extracted by ultrasonication for 10 min in an ice water bath. All extracts after sonication were placed once again in a refrigerator at −40°C for 2 h and then centrifuged at 4°C and 15,620×*g* for 10 min. Then, the supernatant was aspirated by using a disposable syringe and filtered through 0.22 μm microfilters. Then, 150 μL supernatants were transferred into LC brown vials for LC-MS analysis.

The final samples were run on an ACQUITY UPLC I-Class system (Waters Corporation, USA) in high-performance liquid chromatography with a QExactive Plus mass spectrometer. An ACQUITY UPLC HSS T3 column (1.8 μm, 100 mm×2.1 mm) was applied for detection. The running conditions were as follows: column temperature, 45°C; flow rate, 0.35 mL min^{-1}; injection volume, 5 μL; mobile phase A, water with 0.1% formic acid; and mobile phase B, acetonitrile. The elution gradient was as follows: 0 min, 5% B; 2 min, 5% B; 4 min, 30% B; 8 min, 50% B; 10 min, 80% B; 14 min, 100% B; 15 min, 100% B; 15.1 min, 5% B and 16 min, 5% B. Both positive and negative modes were employed for signal acquisition.

In the next step, metabolites were further identified by Progenesis QI Software (Waters Corporation) and databases (http://www.hmdb.ca, http://www.lipidmaps.org, etc.). OPLS-DA was conducted for the metabolic alterations in the comparison between groups. According to the statistically significant variable importance in the projection (VIP) values (VIP values>1), differential metabolites were selected, and correlation analyses were performed. The R package was applied for the comparison of representative metabolites.

ITS sequencing

DNA was extracted from human and mouse fecal samples of different groups by a DNeasy PowerSoil Pro kit (QIAGEN, USA) (Weinmaier et al., 2023), and the purity and concentration of DNA were further determined by agarose gel electrophoresis and NanoDrop (Thermo Fisher Scientific, USA). The ITS1 variable regions were amplified by polymerase chain reaction (PCR) with the forward primer ITS1F (5′-CTTGGTCATTTAGAGGAAGTAA-3′) and reverse primer ITS2 (5′-GCTGCGTTCTTCATCGATGC-3′). Following PCR purification, amplification, and repurification, the concentrations of the final amplicon were terminated with a Qubit dsDNA Assay Kit (Thermo Fisher Scientific). The sequencing products were then conducted via Illumina NovaSeq 6000 with 250 bp paired-end reads. Trimmed by Cutadapt software and modified by DADA2, sequencing reads were annotated and aligned against the Unite database by the QIIME2 package. By the R package and ANOVA/Kruskal-Wallis statistical test, α-diversity (including Chao1 index, Simpson index and Shannon index) and β-diversity (including Bray-Ccurtis- and Binary-jaccard-based PCoA) were further evaluated. The LefSe method was applied to compare the taxonomy abundance spectrum. Differential species between multiple groups were compared by Kruskal-Wallis nonparametric analysis. Using the R package, indicator species analysis was performed by calculating each ASV across all samples, while the random forest models were built on the importance of the top 30 genera.

Transcriptome sequencing

RNA extraction from the colon was performed using the RNeasy Mini Kit (QIAGEN). Construction of the transcriptomic library was conducted using the VAHTS Universal V5 RNA-seq Library Prep Kit, following the manufacturer's protocols. Paired-end 150 bp reads were produced by the Illumina Novaseq 6000 sequencing platform, and then clean reads were obtained by Fastp software. HISAT2 software calculated the FPKM to map the comparison of the reference genome. The threshold of differentially expressed gene (DEG)screening was defined as *Q* value<0.05 and $|\log_2\text{Foldchange}| \geqslant 0.0$. Hierarchical clustering analysis was applied by using the R package (3.2.0).

Fungal intervention and verification

Animal models were established as indicated above until the liver pathological state reached LC status. At 4 months, LC mice were administrated with 0.2 mL 1×10^8 CFU ml^{-1} *C. albicans*, *S. cerevisiae*, and 0.2 mL NS twice a week, respectively. 2 months later, liver cancers of mice were monitored and then the 6.5-month-old mice were sacrificed for collecting samples for further studies. Not only H&E staining, Ki-67 and F4/80 IHC staining of livers, but also H&E staining, occluding and ZO-1 IF staining of colons were performed for verification.

Statistical analysis

All data are expressed as the mean±SEM. GraphPad Prism 6 (GraphPad Software) was used to analyze the data, and

https://doi.org/10.1007/s11427-023-2458-1

P values<0.05 were regarded as statistically significant. Multiple group comparisons were calculated by one-way ANOVA with the LSD post hoc test (normally distributed) or chi-square test (abnormally distributed). Relationships among the gut mycobiota and metabolites were assayed using Spearman's rank correlation analysis.

Compliance and ethics

The author(s) declare that they have no conflict of interest. Our research was approved by the Animal Experimental Ethical Inspection of the First Affiliated Hospital, Zhejiang University School of Medicine (Reference Number: 2022-1071), and the Clinical Research Ethics Committee of the First Affiliated Hospital, College of Medicine, Zhejiang University (IIT20220494B).

Acknowledgement

This work was supported by the National Natural Science Foundation of China (81790631), the National Key Research and Development Program of China (2022YFC3602000), the Shandong Provincial Laboratory Project (SYS202202) and Research Project of Jinan Micro-ecological Biomedicine Shandong Laboratory (JNL-2022009B, JNL-2022047D).

References

Acharya, C., and Bajaj, J.S. (2021). Chronic liver diseases and the microbiome—translating our knowledge of gut microbiota to management of chronic liver disease. Gastroenterol 160, 556–572.

Albhaisi, S., Shamsaddini, A., Fagan, A., McGeorge, S., Sikaroodi, M., Gavis, E., Patel, S., Davis, B.C., Acharya, C., Sterling, R.K., et al. (2021). Gut microbial signature of hepatocellular cancer in men with cirrhosis. Liver Transpl 27, 629–640.

Augimeri, G., Fiorillo, M., Morelli, C., Panza, S., Giordano, C., Barone, I., Catalano, S., Sisci, D., Andò, S., and Bonofiglio, D. (2023). The ω-3 docosahexaenoyl ethanolamide reduces CCL5 secretion in triple negative breast cancer cells affecting tumor progression and macrophage recruitment. Cancers 15, 819.

Bajaj, J.S., Liu, E.J., Kheradman, R., Fagan, A., Heuman, D.M., White, M., Gavis, E.A., Hylemon, P., Sikaroodi, M., and Gillevet, P.M. (2018). Fungal dysbiosis in cirrhosis. Gut 67, 1146–1154.

Bi, C., Xiao, G., Liu, C., Yan, J., Chen, J., Si, W., Zhang, J., and Liu, Z. (2021). Molecular immune mechanism of intestinal microbiota and their metabolites in the occurrence and development of liver cancer. Front Cell Dev Biol 9, 702414.

Chappell, G., Kutanzi, K., Uehara, T., Tryndyak, V., Hong, H.H., Hoenerhoff, M., Beland, F.A., Rusyn, I., and Pogribny, I.P. (2014). Genetic and epigenetic changes in fibrosis-associated hepatocarcinogenesis in mice. Intl J Cancer 134, 2778–2788.

Chen, H.N., Chen, Y., Zhou, Z.G., Wei, Y., and Huang, C. (2019). A novel role for ketoconazole in hepatocellular carcinoma treatment: linking PTGS2 to mitophagy machinery. Autophagy 15, 733–734.

Chen, W., Wen, L., Bao, Y., Tang, Z., Zhao, J., Zhang, X., Wei, T., Zhang, J., Ma, T., Zhang, Q., et al. (2022). Gut flora disequilibrium promotes the initiation of liver cancer by modulating tryptophan metabolism and up-regulating SREBP2. Proc Natl Acad Sci USA 119, e2203894119.

Dapito, D.H., Mencin, A., Gwak, G.Y., Pradere, J.P., Jang, M.K., Mederacke, I., Caviglia, J.M., Khiabanian, H., Adeyemi, A., Bataller, R., et al. (2012). Promotion of hepatocellular carcinoma by the intestinal microbiota and TLR4. Cancer Cell 21, 504–516.

de Bus, I., van Krimpen, S., Hooiveld, G.J., Boekschoten, M.V., Poland, M., Witkamp, R.F., Albada, B., and Balvers, M.G.J. (2021). Immunomodulating effects of 13- and 16-hydroxylated docosahexaenoyl ethanolamide in LPS stimulated RAW264.7 macrophages. Biochim Biophys Acta Mol Cell Biol Lipids 1866, 158908.

Deng, T., Li, J., He, B., Chen, B., Liu, F., Chen, Z., Zheng, J., Shi, Z., Zhang, T., Deng, L., et al. (2022). Gut microbiome alteration as a diagnostic tool and associated with inflammatory response marker in primary liver cancer. Hepatol Int 16, 99–111.

Gao, Y., Wang, J., Zhao, M., Xia, T., Liu, Q., Chen, N., Liao, W., Zeng, Z., You, F., and Zeng, J. (2022). Atractylenolide III attenuates angiogenesis in gastric precancerous lesions through the downregulation of δ-like ligand 4. Front Pharmacol 13, 797805.

Garcia-Hernandez, V., Quiros, M., and Nusrat, A. (2017). Intestinal epithelial claudins: expression and regulation in homeostasis and inflammation. Ann New York Acad Sci 1397, 66–79.

Hartmann, P., and Schnabl, B. (2023). Fungal infections and the fungal microbiome in hepatobiliary disorders. J Hepatol 78, 836–851.

Iida, N., Mizukoshi, E., Yamashita, T., Yutani, M., Seishima, J., Wang, Z., Arai, K., Okada, H., Yamashita, T., Sakai, Y., et al. (2021). Chronic liver disease enables gut Enterococcus faecalis colonization to promote liver carcinogenesis. Nat Cancer 2, 1039–1054.

Jia, W., Li, Y., Cheung, K.C.P., and Zheng, X. (2023). Bile acid signaling in the regulation of whole body metabolic and immunological homeostasis. Sci China Life Sci doi: 10.1007/s11427-023-2353-0.

Jiang, T.T., Shao, T.Y., Ang, W.X.G., Kinder, J.M., Turner, L.H., Pham, G., Whitt, J., Alenghat, T., and Way, S.S. (2017). Commensal fungi recapitulate the protective benefits of intestinal bacteria. Cell Host Microbe 22, 809–816.e4.

Kah, J., Wüstenberg, A., Keller, A.D., Sirma, H., Montalbano, R., Ocker, M., Volz, T., Dandri, M., Tiegs, G., and Sass, G. (2012). Selective induction of apoptosis by HMG-CoA reductase inhibitors in hepatoma cells and dependence on p53 expression. Oncol Rep 28, 1077–1083.

Kala, K., Pająk, W., Sułkowska-Ziaja, K., Krakowska, A., Lazur, J., Fidurski, M., Marzec, K., Zięba, P., Fijałkowska, A., Szewczyk, A., et al. (2022). *Hypsizygus marmoreus* as a source of indole compounds and other bioactive substances with health-promoting activities. Molecules 27, 8917.

Lang, S., Duan, Y., Liu, J., Torralba, M.G., Kuelbs, C., Ventura-Cots, M., Abraldes, J.G., Bosques-Padilla, F., Verna, E.C., Brown, R.S., et al. (2020). Intestinal fungal dysbiosis and systemic immune response to fungi in patients with alcoholic hepatitis. Hepatol 71, 522–538.

Li, M., Yang, Z., Song, Z., Bo, C., Wang, S., and Jia, Q. (2023a). ATM deficiency aggravates the progression of liver fibrosis induced by carbon tetrachloride in mice. Toxicol 484, 153397.

Li, W., Xiao, J., Zhou, X., Xu, M., Hu, C., Xu, X., Lu, Y., Liu, C., Xue, S., Nie, L., et al. (2015). STK4 regulates TLR pathways and protects against chronic inflammation-related hepatocellular carcinoma. J Clin Invest 125, 4239–4254.

Li, Y., Wang, J., Li, L., Song, W., Li, M., Hua, X., Wang, Y., Yuan, J., and Xue, Z. (2023b). Natural products of pentacyclic triterpenoids: from discovery to heterologous biosynthesis. Nat Prod Rep 40, 1303–1353.

Liang, S., Ma, H.Y., Zhong, Z., Dhar, D., Liu, X., Xu, J., Koyama, Y., Nishio, T., Karin, D., Karin, G., et al. (2019). NADPH oxidase 1 in liver macrophages promotes inflammation and tumor development in mice. Gastroenterol 156, 1156–1172.e6.

Ling, Z., Xiao, H., and Chen, W. (2022). Gut microbiome: the cornerstone of life and health. Adv Gut Microbiome Res 2022, 1–3.

Liu, B., Zhou, Z., Jin, Y., Lu, J., Feng, D., Peng, R., Sun, H., Mu, X., Li, C., and Chen, Y. (2022a). Hepatic stellate cell activation and senescence induced by intrahepatic microbiota disturbances drive progression of liver cirrhosis toward hepatocellular carcinoma. J Immunother Cancer 10, e003069.

Liu, J., Geng, W., Sun, H., Liu, C., Huang, F., Cao, J., Xia, L., Zhao, H., Zhai, J., Li, Q., et al. (2022b). Integrative metabolomic characterisation identifies altered portal vein serum metabolome contributing to human hepatocellular carcinoma. Gut 71, 1203–1213.

Liu, Z., Li, Y., Li, C., Lei, G., Zhou, L., Chen, X., Jia, X., and Lu, Y. (2022c). Intestinal *Candida albicans* promotes hepatocarcinogenesis by up-regulating NLRP6. Front Microbiol 13, 812771.

Llovet, J.M., Kelley, R.K., Villanueva, A., Singal, A.G., Pikarsky, E., Roayaie, S., Lencioni, R., Koike, K., Zucman-Rossi, J., and Finn, R.S. (2021). Hepatocellular carcinoma. Nat Rev Dis Primers 7, 6.

Llovet, J.M., Zucman-Rossi, J., Pikarsky, E., Sangro, B., Schwartz, M., Sherman, M., and Gores, G. (2016). Hepatocellular carcinoma. Nat Rev Dis Primers 2, 16018.

Ma, J., Wang, R., Chen, Y., Wang, Z., and Dong, Y. (2023). 5-HT attenuates chronic stress-induced cognitive impairment in mice through intestinal flora disruption. J Neuroinflamm 20, 23.

Manogaran, S., Kilavan Packiam, K., Senthil Kumar, P., Rangasamy, G., and Saravanan, A. (2023). Utilization of industrial waste-liquid cheese whey for the batch fermentation of lovastatin using *Fusarium nectrioides* (MH173849) an endophytic fungus: screening, production and characterization. Chemosphere 318, 137947.

Naglik, J.R., Fidel Jr, P.L., and Odds, F.C. (2008). Animal models of mucosal *Candida* infection. Fems Microbiol Lett 283, 129–139.

Park, C.G., Kim, J.J., and Kim, H.K. (2020). Lipase-mediated synthesis of ricinoleic acid vanillyl ester and evaluation of antioxidant and antibacterial activity. Enzyme Microb Tech 133, 109454.

Qi, X., Chen, S., He, H., Wen, W., and Wang, H. (2021). The role and potential application of extracellular vesicles in liver cancer. Sci China Life Sci 64, 1281–1294.

Ren, Z., Li, A., Jiang, J., Zhou, L., Yu, Z., Lu, H., Xie, H., Chen, X., Shao, L., Zhang, R.,

et al. (2019). Gut microbiome analysis as a tool towards targeted non-invasive biomarkers for early hepatocellular carcinoma. Gut 68, 1014–1023.
Rey, S., Quintavalle, C., Burmeister, K., Calabrese, D., Schlageter, M., Quagliata, L., Cathomas, G., Diebold, J., Molinolo, A., Heim, M.H., et al. (2017). Liver damage and senescence increases in patients developing hepatocellular carcinoma. J Gastro Hepatol 32, 1480–1486.
Roderburg, C., and Luedde, T. (2014). The role of the gut microbiome in the development and progression of liver cirrhosis and hepatocellular carcinoma. Gut Microbes 5, 441–445.
Sanada, S., Suzuki, T., Nagata, A., Hashidume, T., Yoshikawa, Y., and Miyoshi, N. (2020). Intestinal microbial metabolite stercobilin involvement in the chronic inflammation of *ob*/*ob* mice. Sci Rep 10, 6479.
Szóstak, N., Figlerowicz, M., and Philips, A. (2023). The emerging role of the gut mycobiome in liver diseases. Gut Microbes 15, 2211922.
Thoen, L.F.R., Guimarães, E.L.M., Dollé, L., Mannaerts, I., Najimi, M., Sokal, E., and van Grunsven, L.A. (2011). A role for autophagy during hepatic stellate cell activation. J Hepatol 55, 1353–1360.
Tonon, M., Angeli, P., and Piano, S. (2021). Bacterial infections in cirrhosis. Infect Microbes Dis 3, 117–124.
Trebicka, J., Bork, P., Krag, A., and Arumugam, M. (2021). Utilizing the gut microbiome in decompensated cirrhosis and acute-on-chronic liver failure. Nat Rev Gastroenterol Hepatol 18, 167–180.
Villanueva, A. (2019). Hepatocellular carcinoma. N Engl J Med 380, 1450–1462.
Wang, C., Zhou, X., Wang, M., and Chen, X. (2021). The impact of SARS-CoV-2 on the human immune system and microbiome. Infect Microbes Dis 3, 14–21.
Wang, N., Liu, H., Liu, G., Li, M., He, X., Yin, C., Tu, Q., Shen, X., Bai, W., Wang, Q., et al. (2020a). Yeast β-D-glucan exerts antitumour activity in liver cancer through impairing autophagy and lysosomal function, promoting reactive oxygen species production and apoptosis. Redox Biol 32, 101495.
Wang, W., Dong, X.X., Liu, Y., Ni, B., Sai, N., You, L., Sun, M., Yao, Y., Qu, C., Yin, X., et al. (2020b). Itraconazole exerts anti-liver cancer potential through the Wnt, PI3K/AKT/mTOR, and ROS pathways. Biomed Pharmacother 131, 110661.
Weinmaier, T., Conzemius, R., Bergman, Y., Lewis, S., Jacobs, E.B., Tamma, P.D., Materna, A., Weinberger, J., Beisken, S., and Simner, P.J. (2023). Validation and application of long-read whole-genome sequencing for antimicrobial resistance gene detection and antimicrobial susceptibility testing. Antimicrob Agents Chemother 67, e0107222.
Wu, H.Y., Mortensen, U.H., Chang, F.R., and Tsai, H.Y. (2023). Whole genome sequence characterization of *Aspergillus terreus* ATCC 20541 and genome comparison of the fungi *A. terreus*. Sci Rep 13, 194.
Xue, C., Jia, J., Gu, X., Zhou, L., Lu, J., Zheng, Q., Su, Y., Zheng, S., and Li, L. (2022). Intratumoral bacteria interact with metabolites and genetic alterations in hepatocellular carcinoma. Sig Transduct Target Ther 7, 335.
Yu, L.X., and Schwabe, R.F. (2017). The gut microbiome and liver cancer: mechanisms and clinical translation. Nat Rev Gastroenterol Hepatol 14, 527–539.
Zeng, S., Hartmann, P., Park, M., Duan, Y., Lang, S., Llorente, C., Wang, Y., Cabré, N., Fouts, D.E., Bacher, P., et al. (2023a). Malassezia restricta promotes alcohol-induced liver injury. Hepatol Commun 7, e0029.
Zeng, S., Rosati, E., Saggau, C., Messner, B., Chu, H., Duan, Y., Hartmann, P., Wang, Y., Ma, S., Huang, W.J.M., et al. (2023b). *Candida albicans*-specific Th17 cell-mediated response contributes to alcohol-associated liver disease. Cell Host Microbe 31, 389–404.e7.
Zhang, E.B., Zhang, X., Wang, K., Zhang, F., Chen, T.W., Ma, N., Ni, Q.Z., Wang, Y.K., Zheng, Q.W., Cao, H.J., et al. (2021). Antifungal agent Terbinafine restrains tumor growth in preclinical models of hepatocellular carcinoma via AMPK-mTOR axis. Oncogene 40, 5302–5313.
Zhang, F., Aschenbrenner, D., Yoo, J.Y., and Zuo, T. (2022a). The gut mycobiome in health, disease, and clinical applications in association with the gut bacterial microbiome assembly. Lancet Microbe 3, e969–e983.
Zhang, H., Wei, Y., Jia, H., Chen, D., Tang, X., Wang, J., Chen, M., and Guo, Y. (2022b). Immune activation of characteristic gut mycobiota *Kazachstania pintolopesii* on IL-23/IL-17R signaling in ankylosing spondylitis. Front Cell Infect Microbiol 12, 1035366.
Zhang, L., Chen, C., Chai, D., Li, C., Qiu, Z., Kuang, T., Liu, L., Deng, W., and Wang, W. (2023). Characterization of the intestinal fungal microbiome in patients with hepatocellular carcinoma. J Transl Med 21, 126.